Research Article

Synthesis and Morphological Transformation of Conjugated Amphiphilic Diblock Copolymers in Mixed Solvents

Yang-Yen Yu,[1,2,3] Chung-Yi Hsu,[1] and Guo-You Li[1]

[1] Department of Materials Engineering, Ming Chi University of Technology, 84 Gungjuan Road, Taishan District, New Taipei City 24301, Taiwan
[2] Center for Thin Film Technologies and Applications, Ming Chi University of Technology, 84 Gungjuan Road, Taishan, New Taipei City 243, Taiwan
[3] Battery Research Center of Green Energy, Ming Chi University of Technology, 84 Gungjuan Road, Taishan District, New Taipei City 24301, Taiwan

Correspondence should be addressed to Yang-Yen Yu; yyyu@mail.mcut.edu.tw

The synthesis, morphological transformation, and photophysical properties of a rod-coil block copolymer, poly[2,7-(9,9-dihexyl-fluorene)]-block-poly(2-vinylpyridine) (PF-b-P2VP), with P2VP coils of various lengths in a mixed methanol/tetrahydrofuran (MeOH/THF) solvent are reported. Various morphological structures of PF-b-P2VP aggregates, including spheres, short worm-like structures, long cylinders, and large compound micelles (LCMs), were observed after varying the coil length of PF-b-P2VP and the selectivity of mixed solvents. These aggregated structures demonstrated considerable variation with regard to optical absorption, fluorescence, and the PL quantum yield of rod-coil copolymers. The degree of hypsochromic spectral shift was enhanced as the length of P2VP coils and the content of poor solvent increased. This study reveals the influence of coil length and selectivity of solvents on the morphology and the optical characteristics of rod-coil amphiphilic copolymers.

1. Introduction

The self-assembly of amphiphilic block copolymers (ABCs) is considered a promising approach to synthesize nanostructured or hierarchical materials with novel morphological and physical properties for advanced applications in areas such as electronics, optoelectronics, biotechnology, and environmental technology [1–13]. The morphology of amphiphilic block copolymers can be manipulated using different driving forces, including relative block length, block polarity, volume fraction, and temperature [14–16]. Recently, amphiphilic rod-coil diblock copolymers [17, 18] have attracted considerable attention, as they produce novel self-organizing structures in the form of stiff rod-like segments, such as helical [19] and π-conjugation polymers [20–25]. In the past 5 years, a great number of new π-conjugated polymers have been synthesized and used in various biological applications such as sensing and imaging agents. These studies have focused on highly sensitive diagnosis of pathogenic microorganisms and tumor cells and detection of disease-related biomarkers. Beyond sensing, fluorescence imaging in vitro has also been successfully achieved. Besides, these materials have also attracted much attention for biomedical applications, such as monitoring drug delivery and release, gene delivery, drug screening, and anti-microorganism and anticancer therapies [26–28].

Rod-coil block copolymers containing π-conjugation chains are of particular importance because conjugated homopolymers are among the most promising candidates for low-cost, large-area, flexible organic electronics [29]. The high immiscibility and stiffness asymmetry between rigid conjugated rods and flexible coil segments significantly influence the molecular packing of polymers, leading to self-organized aggregation. The aggregation of rod-like conjugated chains enables the production of a wide variety of

supramolecular structures at nanoscale dimensions, including lamellar, spherical, cylindrical, vesicular, and worm-like structures that further influence electronic and photophysical properties [17, 18]. Polyfluorene (PF) and its derivatives have been widely used for polymer light-emitting diodes, owing to their high fluorescence quantum yield and good charge transport ability [30–33]. Although PF is a promising material for light-emitting diodes, PF chains tend to stack cofacially and form excimers due to intermolecular π-π interaction, which results in nonradiative decay and a subsequent reduction in the performance of devices. A diblock architecture is one possible solution to lower the intermolecular interaction in PF and suppress the formation of excimers [34]. Moreover, the photophysical properties are possibly influenced strongly by variations in the morphology of rod-coil copolymers. Rod-coil block copolymers with fluorene-based segments have been reported by several groups [35–37]. The importance of the morphological transformation of rod-coil poly[2,7-(9,9-dihexylfluorene)]-*block*-poly(2-vinylpyridine) (PF-b-P2VP) via selective solvents on optical characteristics has been demonstrated [22]. Diverse morphological and optical properties can be induced in the aggregate by changing the MeOH/THF ratio. However, the means by which the length of coil segments and solvent quality influence the morphology of PF-b-P2VP have not yet been fully explored.

This study demonstrates the synthesis, morphology, and photophysical properties of amphiphilic PF_m-b-$P2VP_n$ at a fixed rod length ($m = 10$) with three different coil lengths ($n = 35, 55, 75$). The chemical structure of the studied polymers and the synthetic scheme for the PF-b-P2VP block copolymer are shown in Scheme 1. By varying the selectivity of the solvents and the annealing temperature, polymers with various aggregation morphologies were induced. This paper reveals the influence of the ratio of poor/good solvents on the morphological and photophysical properties of these diblock copolymers with various coil lengths as well as the spectral stability of PF-b-P2VP. Finally, transmission electron microscopy (TEM), atomic force microscopy (AFM), UV-vis optical absorption, and photoluminescence (PL) spectroscopy were employed to investigate the correlation between optical characterization and morphology.
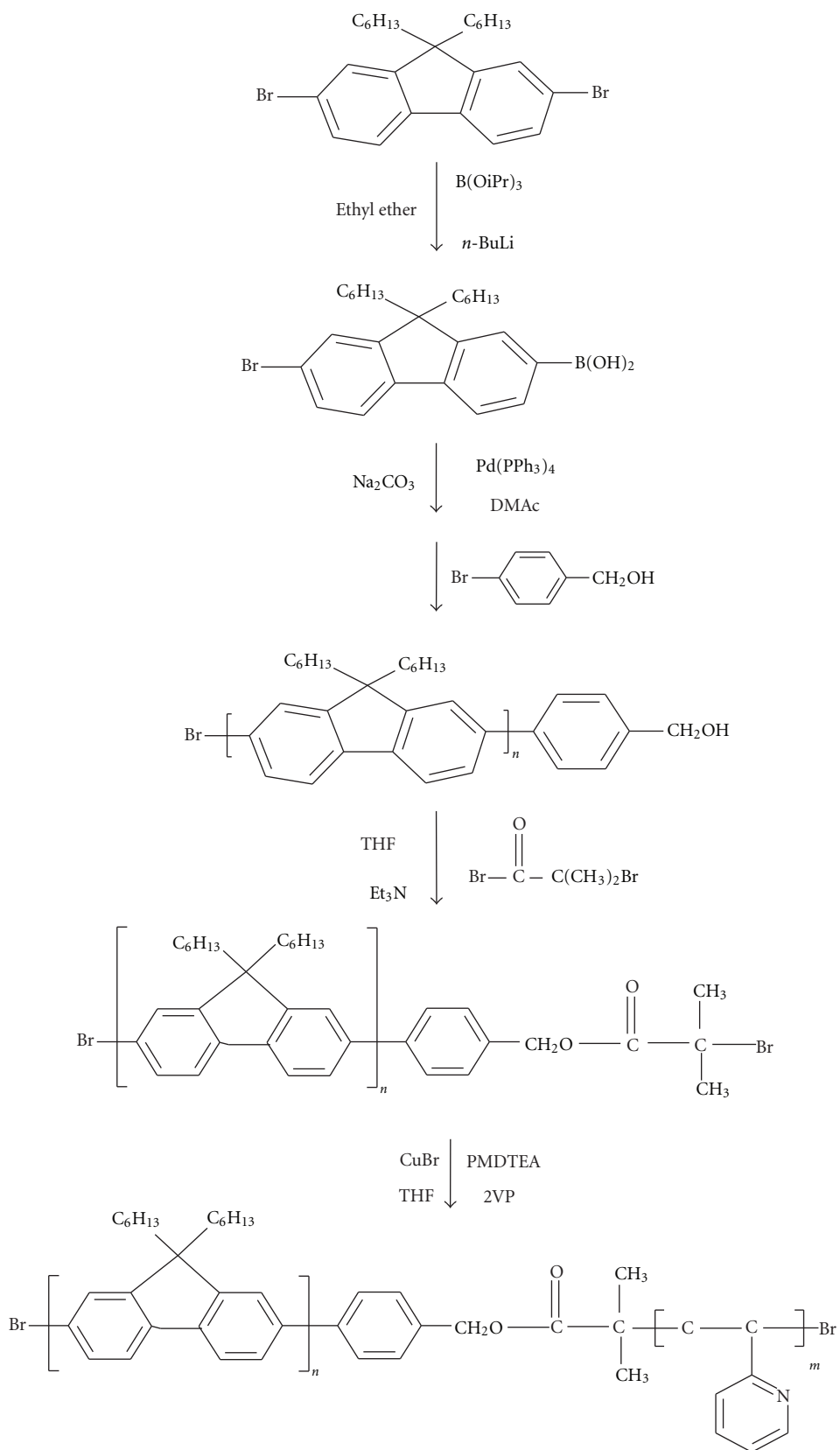
2. Experimental

2.1. Materials. 9,9-dihexyl-2-7-dibromofluorene (F, Aldrich, 97%), 2-Vinylpyridine (2VP, Acros, 97%), copper(I) bromide (CuBr, Aldrich, 99.999%), anhydrous tetrahydrofuran (THF, Echo), N, N, N', N', N''-pentamethyldiethylenetriamine (PMDETA, Aldrich, 99%), anhydrous methyl alcohol (MeOH, Mallinckrodt), n-hexane (Tedia, 95%), Aluminium oxide (50–200 micron, Acros), and chloroform-d (99.8 atm% D, Aldrich) were used as received to prepare the PF-b-P2VP copolymers.

2.2. Synthesis of PF-b-P2VP Copolymers and Preparation of PF-b-P2VP Aggregates in Mixed Solvents. First, α-(4-hydroxymethyl phenyl)-ω-bromo-poly[2,7-(9,9-dihexyl-fluorene)] was synthesized according to the literature [38]. 2-bromo-7-bromohydroxide-9,9-dioctylfluorene was prepared

by boronation of 9,9-dihexyl-2,7-dibromofluorene with tri-isopropyl borate at $-78°C$. The polymerization of the prepared product using a modified Suzuki coupling protocol followed by end capping with bromobenzene yielded α-bromo-ω-phenyl-poly(9,9-dioctylfluorene). Then, a second Suzuki reaction of α-bromo-ω-phenyl-poly(9,9-dioctylfluorene) with an excess of 4-formylphenylboronic acid, now using the well-known toluene-soda two-phase system, yielded almost quantitatively α-(4-formylphenyl)-ω-(phenyl)-poly(2,7-(9,9-dioctylfluorene)). It was then reacted with 2-bromoisobutyl bromide to obtain the polyfluorene macroinitiator, α-{4-[2-(2-bromo-2-methylpropoyloxy)methyl]phenyl}-ω-bromo-poly[2,7-(9,9-dihexyl-fluorene)] (PF-Br). GPC analysis revealed an Mn of 5300 g/mol, which corresponds to ten fluorene repeating units. Finally, poly [2,7-(9,9-dihexylfluorene)]-block-poly(2-Vinylpyridine) (PF-b-P2VP) was synthesized from PF-Br by atom transfer radical polymerization. Taking PF_{10}-b-$P2VP_{75}$ as an example, 300 mg (1 mmol) of PF-Br, 13.4 mg of CuBr (2 mmol), and 1.056 mL of 2-VP (200 mmol) were added to a dry round-bottom flask, and the system was maintained under vacuum for 30 min. 0.02 mL solution of PMDETA (2 mmol) in 2.6 mL of THF was added into the round-bottom flask under a nitrogen atmosphere. The mixture was degassed three times, filled with nitrogen, stirred at ambient temperature for 30 min, and immersed into an oil bath at $120°C$ for 24 h. After cooling to room temperature, the mixture was passed through an Al_2O_3 column to remove the copper catalyst, precipitated into an excess amount of n-Hexane, filtered off, and the remaining product dried under vacuum at $30°C$ to obtain 100 mg of PF-b-P2VP as a black solid (yields: 95%). ^{1}H NMR (CDCl$_3$), P2VP block: δ(ppm) = 8.5–8.0, 7.5–6.0 (4H, pyridine), 3.78 (1H, CH(pyr)-C(O)), 2.3, 1.8 (3H, back-bone). GPC: Mn (PF) = 5300, Mn(P2VP) = 10700, PDI = 1.33 for PF_{10}-b-$P2VP_{35}$; Mn(PF) = 5300, Mn(P2VP) = 11198, PDI = 1.41 for PF_{10}-b-$P2VP_{55}$; Mn(PF) = 5300, Mn(P2VP) = 14900, PDI = 1.26 for PF_{10}-b-$P2VP_{75}$. Moreover, the prepared PF-b-P2VP copolymer solid was dissolved into the mixed MeOH/THF solvents with different volume ratios of MeOH/THF, that is, 0, 10, 25, 50, 75, and 90%. During the experiment, it was found that the block chain length of copolymers dominated the morphologies of copolymer aggregates under a fixed copolymer concentration. The effect of polymer concentration could be neglected. Therefore, the polymer concentration of all solution was maintained at 0.1 wt%.

2.3. Characterization. ^{1}H-NMR spectra of the prepared polymers were performed by a Jeol EX-400 spectrometer. The molecular weight was determined using a GPC instrument equipped with a refractive index detector (Schambeck SFD GmbH, model RI 2000), a Lab Alliance solvent delivery system, and a GPC column (PLgel 5 μm mixed, C and D). Calibration was achieved by injecting polystyrene standard diluted to 0.5 wt% in THF (1 mL/min) at $40°C$. Thermal analyses were carried out on a differential scanning calorimetry (DSC) from TA instruments (TA Q20) with a heating cycle from room temperature to $200°C$ at a heating rate of $20°C$/min and a thermal gravimetric analyzer (TGA) from TA instruments

Scheme 1: Chemical structures of the synthesized PF-b-P2VP rod-coil diblock copolymers.

(TA Q50) with a heating range from room temperature to 900°C at a heating rate of 20°C/min.

The PF-b-P2VP aggregate morphologies were characterized by transmission electron microscopy (TEM) using a JEOL 1210 operating at an acceleration voltage of 100 kV. A drop of the aggregate dispersion was cast onto a 200 mesh copper TEM grid deposited with carbon and dried under vacuum before imaging. The deuterated solvent used for obtaining the spectra was chloroform-d. The AFM data was performed in tapping mode on a Nanoscope DI III multimode AFM. The UV-vis spectra were obtained from polymer thin films prepared on glass by spin coating at a speed of about 1000 rpm using a Jasco Model V-650 spectrometer. The PL spectra were obtained using a Horiba Jobin Yvon Fluoromax-4 Spectrofluorometer with a 450 nm excitation wavelength.

3. Results and Discussion

3.1. Micellar Morphologies. In this study, transmission electron microscopy (TEM) and atomic force microscopy (AFM) are utilized for a more detailed investigation of the morphologies for PF-b-P2VP copolymer in solutions and films, respectively, although dynamic light scattering (DLS) has been applied in the investigation of micellar morphology. However, it is known that DLS is not the appropriate tool to use for gaining deeper information on the morphology of micelles [39]. It is because the analytical result of DLS is obviously affected by the operating condition and calculation method. Besides, DLS cannot provide the real morphologies of micellar aggregation. The selectivity of solvents can be manipulated by selecting solvents with various solubility parameters. The solubility of PF and P2VP is in the range of 18.62–19.02 MPa$^{0.5}$ and 27.6 MPa$^{0.5}$, respectively. The solubility of THF and MeOH is 18.6 and 29.7 MPa$^{0.5}$, respectively. Thus, THF is a suitable solvent for PF and a selective solvent for P2VP. By contrast, methanol is a suitable solvent for P2VP and a selective solvent for PF. Figures 1(a)–1(d) indicate the aggregation behavior of amphiphilic PF$_{10}$-b-P2VP$_{35}$ in a mixed solution of MeOH/THF with various methanol contents: 0, 25, 50, and 75 vol.%. Spherical micelles with a diameter ranging from 50–80 nm were observed in pure THF solution. This is because THF acts as a good solvent for PF, but as a poor solvent for P2VP, resulting in a spherical morphology with a core of P2VP and a corona of PF. By increasing the methanol content to 10 vol.%, some of the spherical micelles began aggregating with one another to form short worm-like structures less than 500 nm in length. Increasing the MeOH content to 25 vol.% resulted in short worm-like structures aggregating to form long three-dimensional network structures, several micrometers in length, due to the ability of these structures to efficiently reduce the interfacial energy of the P2VP core and the PF corona [21]. A further increase in the MeOH content to 50 vol.% resulted in the formation of two morphological structures of PF-b-P2VP aggregate: a spherical micelle with a core of PF and a corona of P2VP and a cylinder with a diameter of 50–100 nm and a length of approximately 300–500 nm. This transformation was due to the expansion of the P2VP core following an increase in MeOH, because MeOH is a good solvent for P2VP,

and the increased selectivity enhances the π-π stacking of the PF segment, resulting in a cylindrical morphology [22]. When the MeOH content exceeded 75 vol.%, all aggregates of PF-b-P2VP formed spherical micelles with a core of PF and a corona of P2VP, because the mixed solution containing a large proportion of MeOH facilitated the stretching of hydrophilic P2VP and the aggregation of the hydrophobic PF. Thus, the P2VP core and PF corona prefer to invert to a PF core and P2VP corona in the presence of large quantities of MeOH [21]. The diameter of the phase-inversed spherical aggregate comprising a PF core and P2VP corona was in the range of 50–80 nm. When the ratio of MeOH/THF increased to 90 vol.%, further aggregation between the small micelles occurred to produce larger spherical aggregates up to 200 nm in diameter, exceeding the size of aggregates comprising a P2VP core and PF corona. This increase in the size of micelles results from the P2VP chain being longer than the PF chain. Figures 1(e) and 1(f) show AFM images of the topography of PF$_{10}$-P2VP$_{35}$ thin films prepared from mixed solutions of MeOH/THF with 25 vol.% and 50 vol.% MeOH, respectively. The images also illustrate the morphologies described previously, in agreement with those obtained from TEM.

As the length of hydrophilic P2VP coils increased from 35–55 nm, a similar morphological transformation was observed. Figures 2(a)–2(d) show TEM images of PF$_{10}$-b-P2VP$_{55}$ in a mixed solution of MeOH/THF. Aggregates of PF$_{10}$-b-P2VP$_{55}$ exhibited spherical micelles, similar to PF$_{10}$-b-P2VP$_{35}$ in pure THF solution. The diameter of the micelles was approximately 70–130 nm, exceeding that of PF$_{10}$-b-P2VP$_{35}$ owing to the longer P2VP chain. With an increase in MeOH content to 10 vol.%, the size of the micelles increased, due to the stretching of the long P2VP chains. The diameter of PF$_{10}$-b-P2VP$_{55}$ ranged from 100–150 nm. Although the PF chains shrank with an increase in MeOH content, P2VP possesses a longer chain than PF; therefore, the volume of P2VP chains increased more than that of PF chains. Although the MeOH content increased to 25 vol.%, large compound micelles (LCMs) with a diameter of 300–500 nm were observed. The formation of LCMs probably arises from the interpenetration of PF into P2VP. An increase in the MeOH content to 50% resulted in the occurrence of phase-inverted micelles with a PF core and P2VP corona, the diameter of which was 50–80 nm. A worm-like morphology was observed with MeOH contents of 75 and 90 vol.% because the aggregation of worm-like micelles reduces the stretching of P2VP, leading to a decreased entropy loss [22]. Figures 2(e) and 2(f) show AFM images of the topography of PF$_{10}$-P2VP$_{55}$ thin films prepared from mixed solutions of MeOH/THF with 25 and 50 vol.% MeOH, respectively. The images exhibit the morphologies described by the TEM analysis.

Figures 3(a)–3(d) show TEM images of PF$_{10}$-b-P2VP$_{75}$ in mixed solvents of MeOH/THF, in which the longer P2VP chains in PF$_{10}$-b-P2VP$_{75}$ provide a stronger driving force to form a long cylindrical morphology, leading to the coexistence of spherical and short worm-like micelle aggregates in the pure THF solution. The diameters of the spherical and worm-like micelles were 120–180 nm and 180–250 nm, respectively. With an increase in MeOH content to 10 vol.% and 25 vol.%, the size of the worm-like micelles
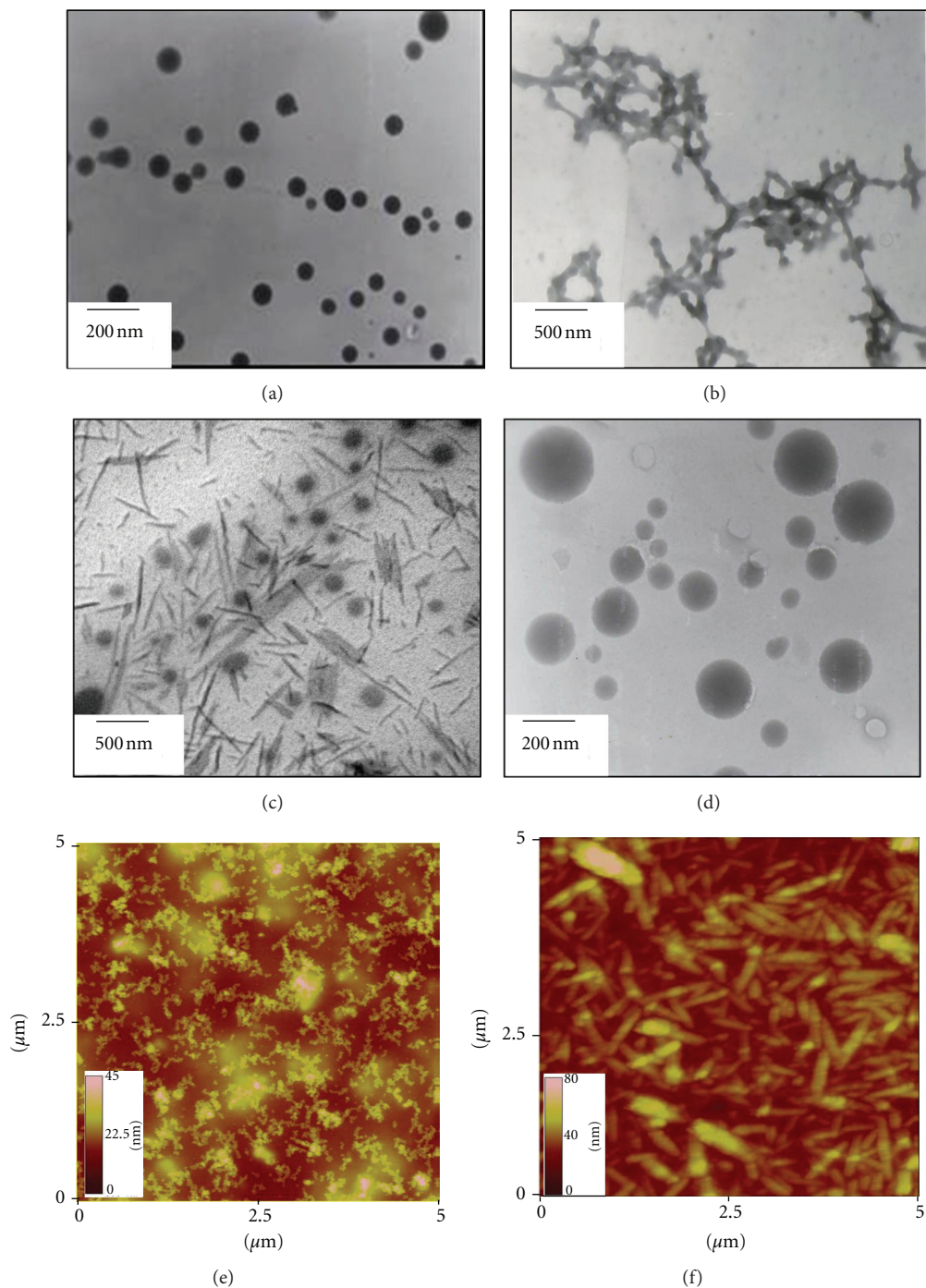
FIGURE 1: TEM images of $(PF)_{10}$-b-$(P2VP)_{35}$ aggregates in dilute solution of MeOH/THF with methanol contents of (a) 0, (b) 25, (c) 50, and (d) 75 vol.%. (e) and(f) show the AFM images for the thin films of PF_{10}-$P2VP_{35}$ prepared at 25 and 50 vol.% MeOH content, respectively.

extended to several micrometers. Increasing the MeOH content to 50 vol.% resulted in the transformation of the worm-like structures into long cylindrical structures with phase-inverted micelles comprising a PF core and P2VP corona. The length of the cylindrical structures was about several to ten micrometers. As the methanol content was increased to 75 vol.%; all aggregates of PF-b-P2VP formed phase-inverted spherical micelles with a core of PF, a corona of P2VP, and

a diameter of approximately 100–150 nm. With a methanol content of 90 vol.%, the swelling of P2VP increased, due to an increase in the solubility of P2VP, resulting in well-dispersed spherical micelles, which increased in size from 150–250 nm. Figures 3(e) and 3(f) show AFM images of the topography of PF_{10}-$P2VP_{55}$ thin films prepared from mixed solutions of MeOH/THF with MeOH content of 50 vol.% and 75 vol.%, respectively. The images also exhibit the long
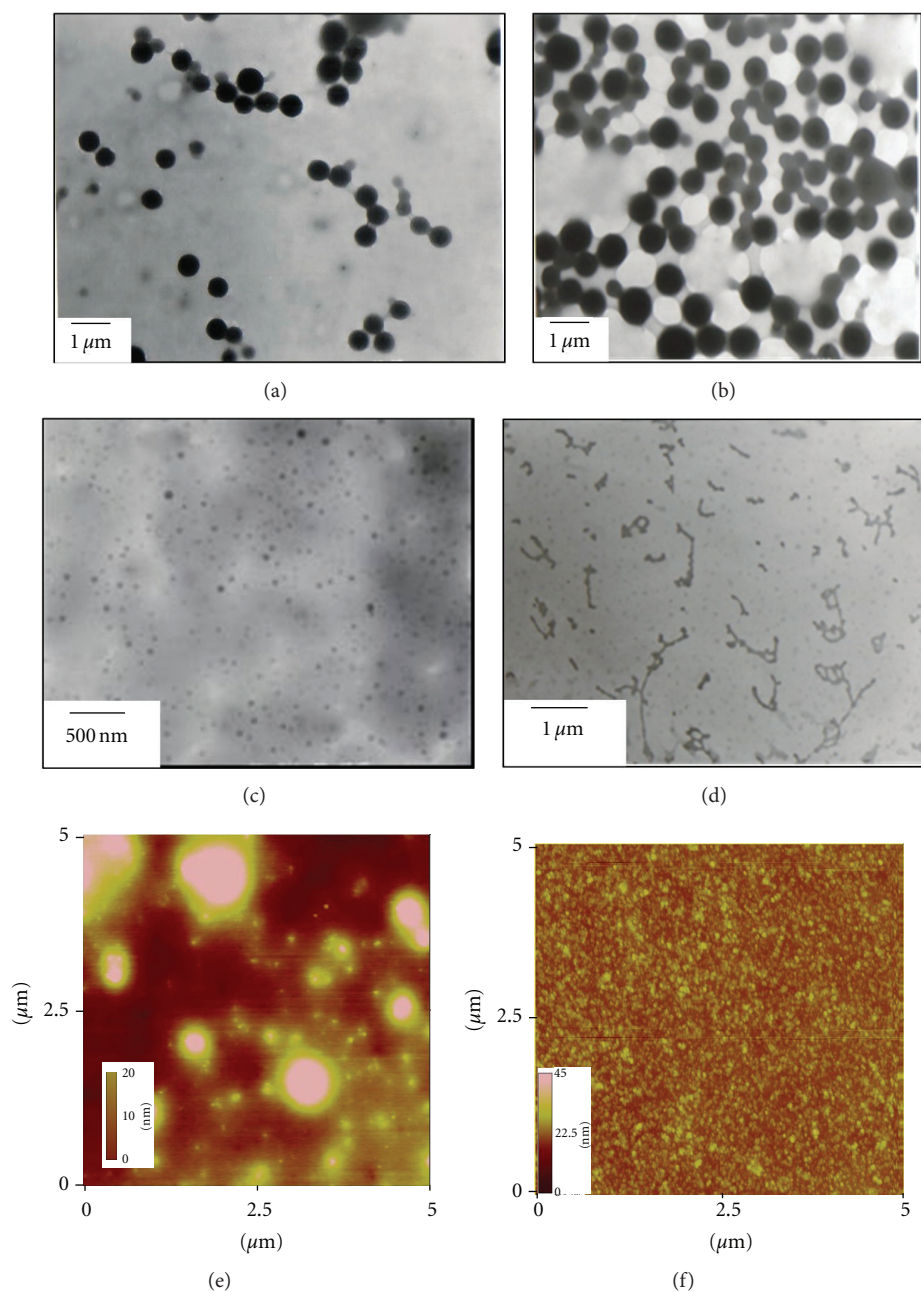
(a)

(b)

(c)

(d)

(e)

(f)

FIGURE 2: TEM images of $(PF)_{10}$-b-$(P2VP)_{55}$ aggregates in dilute solution of MeOH/THF with methanol contents of (a) 0, (b) 25, (c) 50, and (d) 75 vol.%. (e) and (f) show the AFM images for the thin films of PF_{10}-$P2VP_{55}$ prepared at 25 and 50 vol.% MeOH content, respectively.

cylindrical and spherical aggregates described previously.

3.2. Photophysical Properties. Figure 4 shows the optical absorption and photoluminescence (PL) spectra of PF_{10}-$P2VP_{75}$ in a dilute solution of MeOH/THF with MeOH content ranging from 0 to 90 vol.%. The photophysical properties of PF_{10}-$P2VP_{35}$, PF_{10}-$P2VP_{55}$, and PF_{10}-$P2VP_{75}$ are summarized in Table 1. Photophysical analysis shows that both the maximum absorption and photoluminescence spectra of PF_{10}-$P2VP_{35}$, PF_{10}-$P2VP_{55}$, and PF_{10}-$P2VP_{75}$ thin films exhibit a hypsochromic shift with an increase in MeOH

from 0–90 vol.%. The hypsochromic shift is probably due to the fact that the aggregation induced by the poor solvent results in PF segments of reduced coplanarity, leading to a reduction in effective conjugation length [21]. In general, the hypsochromic shift of the absorption spectra is attributed to H-type aggregation, in which conjugation segments are oriented in a parallel direction [22], as shown in Scheme 2. H-type aggregation leads to a blue shift in the absorption spectra and a quenching of fluorescence. The maximum UV-vis peaks of PF_{10}-$P2VP_{35}$, PF_{10}-$P2VP_{55}$, and PF_{10}-$P2VP_{75}$ shifted from 374 nm in pure THF solvent to 362, 362, and 356 nm, respectively, in 90 vol.% MeOH. A similar hypsochromic shift was
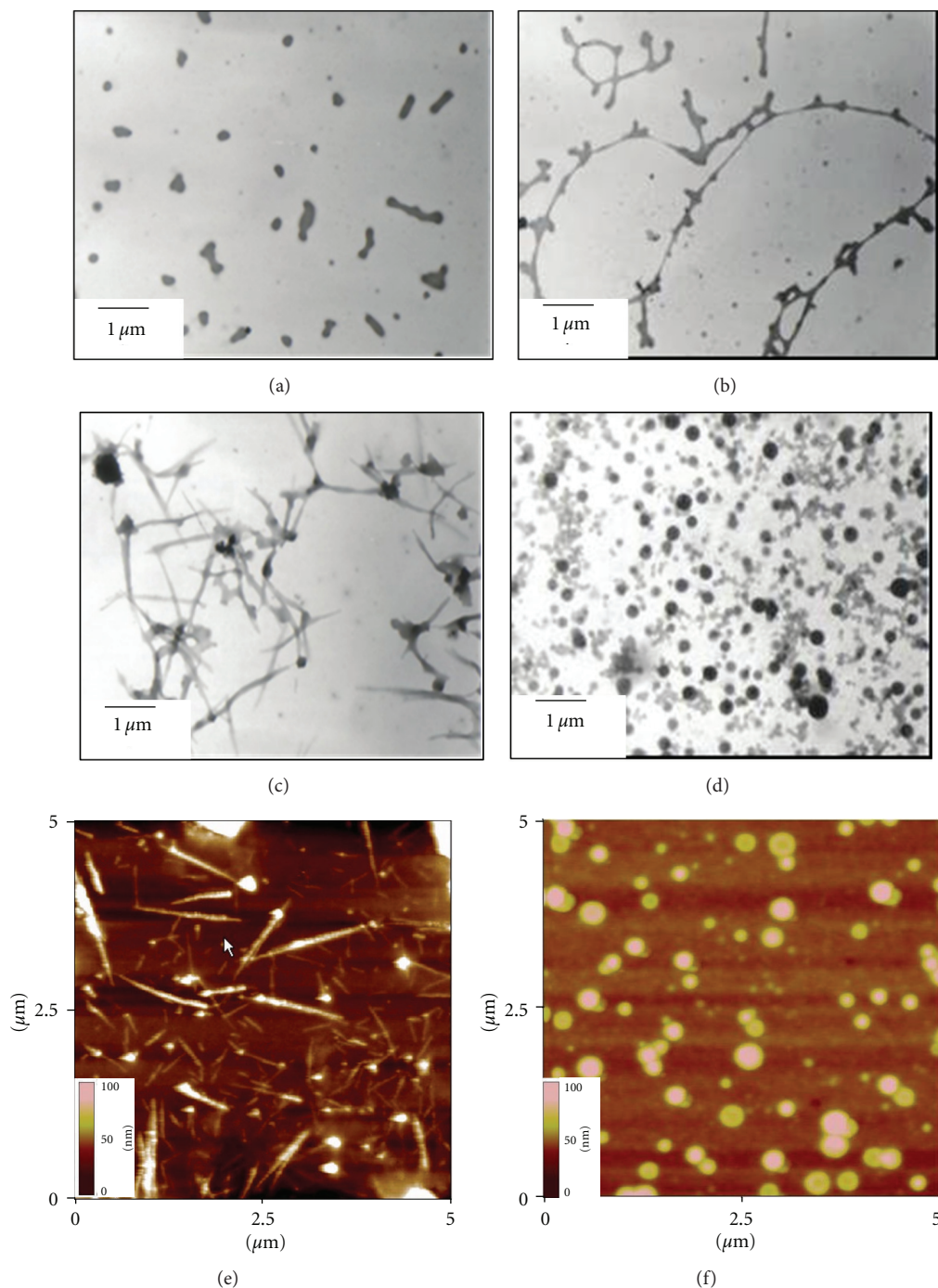
(a)

(b)

(c)

(d)

(e)

(f)

FIGURE 3: TEM images of $(PF)_{10}$-b-$(P2VP)_{75}$ aggregates in dilute solution of MeOH/THF with methanol contents of (a) 0,(b) 25,(c) 50, and (d) 75 vol.%. (e) and (f) show the AFM images for the thin films of PF_{10}-$P2VP_{75}$ prepared at 50 and 75 vol.% MeOH content, respectively.

observed in the PL spectra of PF_{10}-$P2VP_{75}$ with two emission peaks attributed to the radiative decay of singlet excitons. The maximum PL peaks of PF_{10}-$P2VP_{35}$, PF_{10}-$P2VP_{55}$, and PF_{10}-$P2VP_{75}$ shifted from 416 nm, 416 nm, and 415 nm in pure THF solution to 412, 410, and 408 nm, respectively, in 90 vol.% MeOH. Moreover, the PL quantum yields of PF_{10}-$P2VP_{35}$, PF_{10}-$P2VP_{55}$, and PF_{10}-$P2VP_{75}$ decreased from 75,

72, and 71% in pure THF solution to 55, 55, and 45%, respectively, in 90 vol.% MeOH. The degree of hypsochromic shift and the decrease in PL quantum yield increased as the length of P2VP coils and the content of the poor solvent increased, indicating that photophysical properties can be manipulated by the coil length of the P2VP block and the selectivity of the solvents.
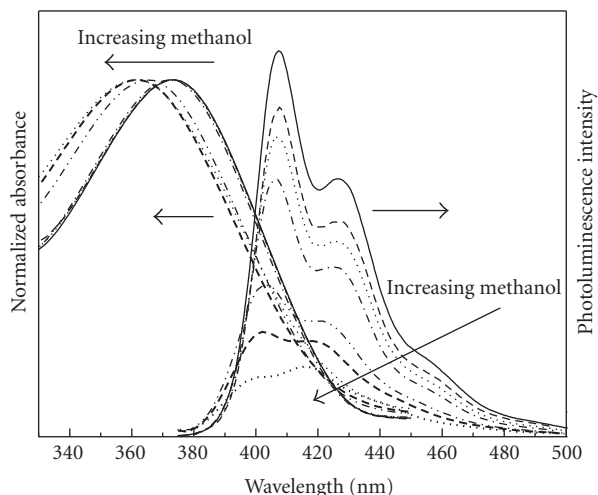
FIGURE 4: Optical absorption and photoluminescence spectra of $(PF)_{10}$-b-$(P2VP)_{75}$ in dilute solution of THF and methanol with methanol contents ranging from 0 to 90 vol.%.
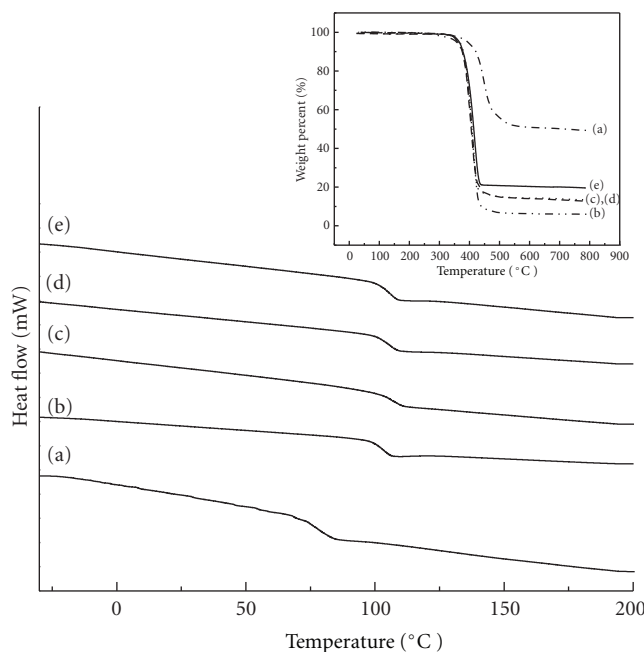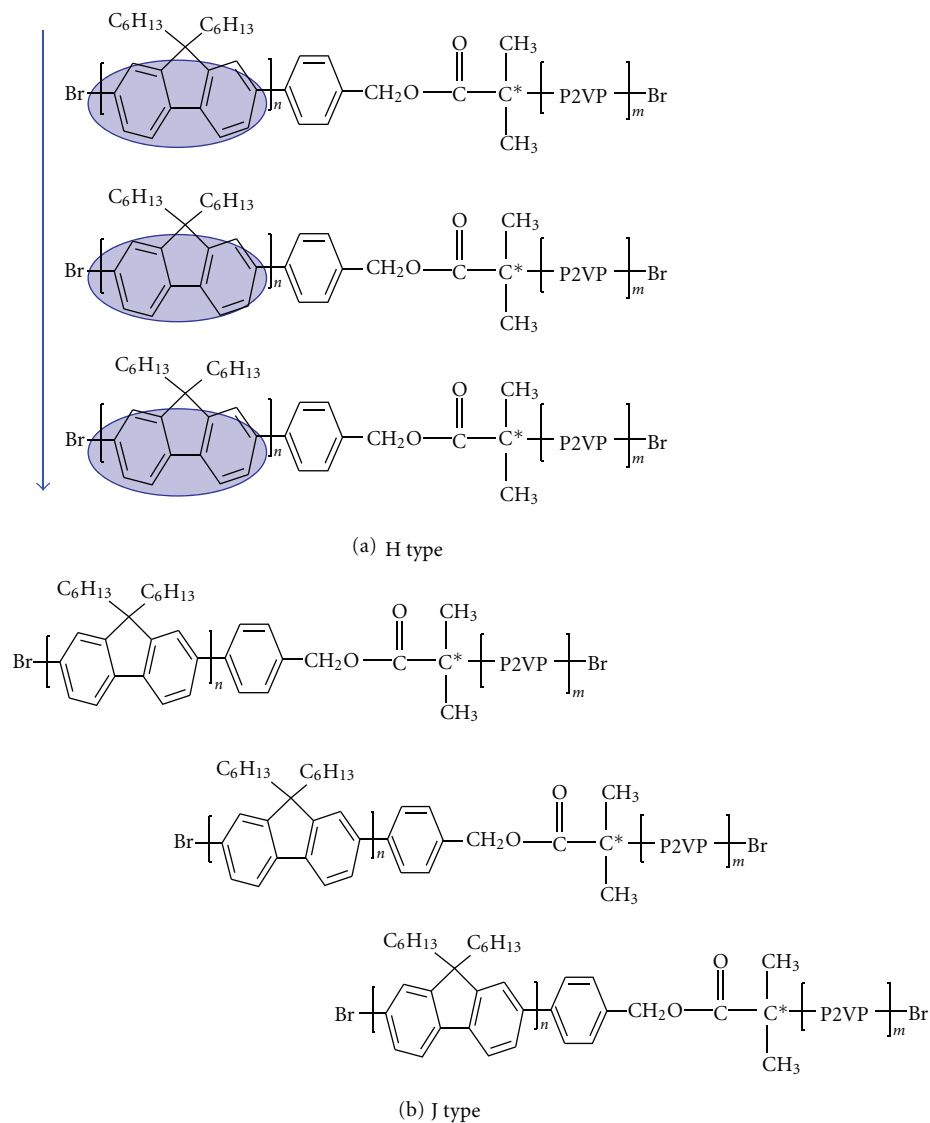

FIGURE 5: DSC thermograms of (a) PF-vinyl macroinitiator, (b) pure P2VP, (c) PF_{10}-b-$P2VP_{35}$, (d) PF_{10}-b-$P2VP_{55}$, and (e) PF_{10}-b-$P2VP_{75}$. The inset shows the TGA curves of the previously mentioned corresponding four polymers.

3.3. Effects of Thermal Annealing on Morphology and Photoluminescence.

The thermal properties of polymers examined by TGA and DSC are shown in Figure 5. In the inset of Figure 5, the thermal degradation temperature (T_d) (weight loss of 5%) of (a) PF-vinyl macroinitiator, (b) pure P2VP, (c) PF_{10}-b-$P2VP_{35}$, (d) PF_{10}-b-$P2VP_{55}$, and (e) PF_{10}-b-$P2VP_{75}$ was observed at 394, 360, 367, 363, and 361°C, respectively. The glass transition temperatures (T_g) of the previously mentioned five polymers were determined from the DSC curves at 86, 109, 112, 109, and 109°C, respectively. The values of T_d and T_g for the prepared di-block copolymers are close to those of the P2VP homopolymer, because the

molecular weight of the P2VP moiety is much greater than that of the PF moiety [22]. Figure 6 shows AFM images of the PF_{10}-$P2VP_{75}$ thin films annealed at room temperature, 80°C, 160°C, and 240°C. At room temperature, the morphology of PF_{10}-$P2VP_{75}$ exhibited a rough surface. With an increase in annealing temperature, surface roughness decreased, presumably because the thermal energy facilitated the movement of polymer chains, which smoothed the surface at higher temperatures. Figures 7 and 8 show the PL spectra of macroinitiators PF-Br and PF_{10}-$P2VP_{75}$, respectively, as a function of annealing time at 120°C. Thin films of PF macroinitiator and PF_{10}-$P2VP_{75}$ were prepared

(a) H type

(b) J type

SCHEME 2: Schematic illustration of (a) H-type and (b) J-type aggregates of diblock PF-b-P2VP copolymers.

TABLE 1: UV-vis and PL characteristics of PF_{10}-b-$P2VP_{35}$, PF_{10}-b-$P2VP_{55}$, and PF_{10}-b-$P2VP_{75}$ thin films in the various ratios of MeOH/THF solvents.

MeOH/THF[1]	PF_{10}-b-$P2VP_{35}$			PF_{10}-b-$P2VP_{55}$			PF_{10}-b-$P2VP_{75}$		
	λ_{max}^{2} (nm)	λ_{max}^{3} (nm)	ψ^{4} (%)	λ_{max}^{2} (nm)	λ_{max}^{3} (nm)	ψ^{4} (%)	λ_{max}^{2} (nm)	λ_{max}^{3} (nm)	ψ^{4} (%)
0/100	374	416	75	374	416	72	374	415	71
10/90	374	416	68	374	416	65	374	414	64
25/75	374	415	60	372	416	58	374	415	56
50/50	372	414	59	372	415	56	370	413	52
75/25	366	413	57	366	412	55	364	411	48
90/10	362	412	55	362	410	55	356	408	45

[1]The various volume ratios of MeOH/THF solvent.
[2]The maximum peaks of UV-vis spectra.
[3]The maximum peaks of PL spectra.
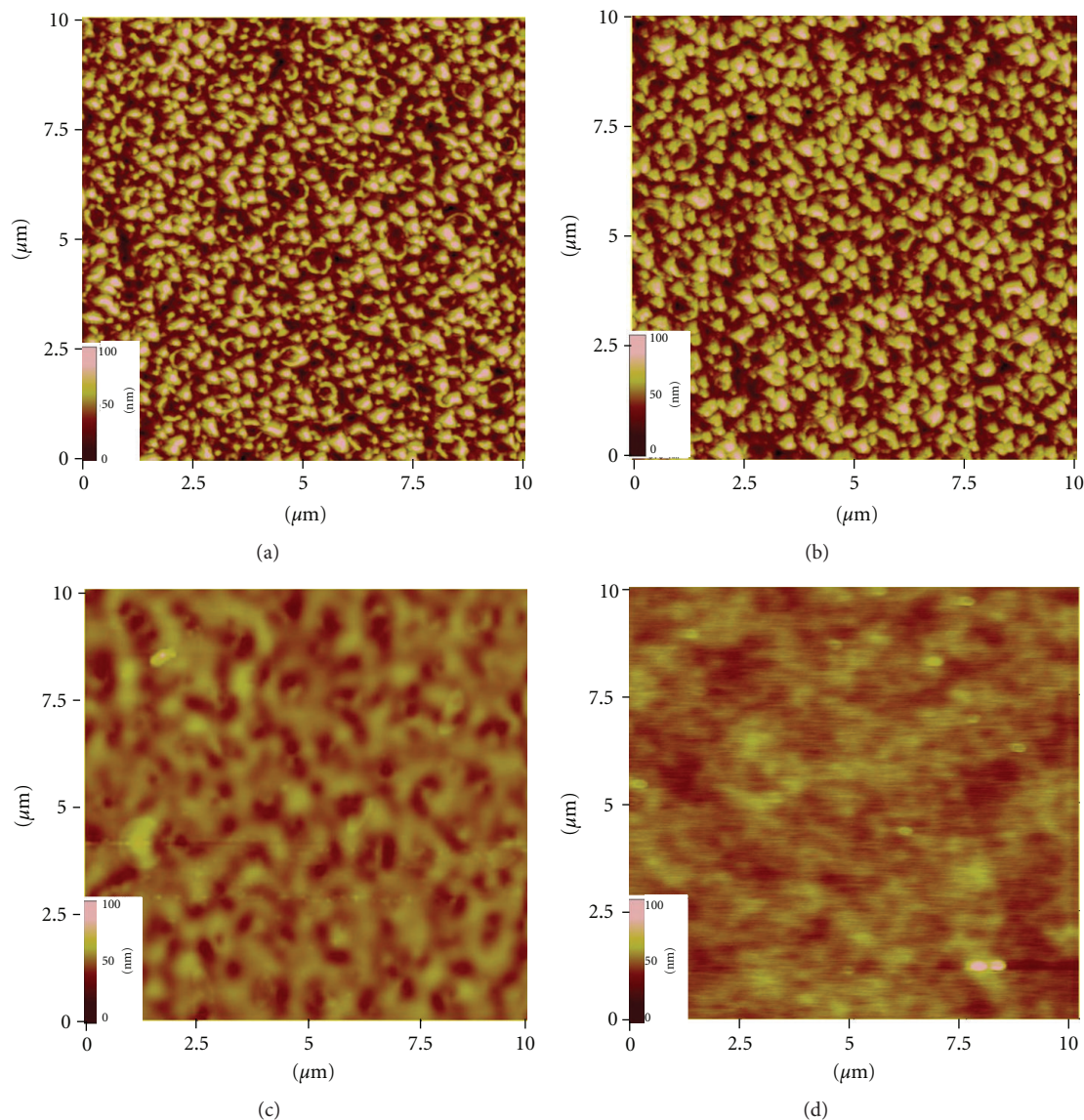[4]The quantum yields of PL.

(a)

(b)

(c)

(d)

FIGURE 6: AFM images of $(PF)_{10}$-b-$(P2VP)_{75}$ obtained at various heating temperature of (a) room temperature, (b) 80°C, (c) 160°C, and (d) 240°C, respectively.

by spin coating and annealing at 120°C in a convection oven for various durations ranging from 0 to 15 h prior to the measurement of PL. Both samples were heat-treated under the same experimental conditions. The results show that the PL emission of PF-Br and PF_{10}-$P2VP_{75}$ increases in the range of 500–600 nm with amplified annealing times, indicating the formation of excimers. The emission of PF-Br at 525 nm is much stronger than that of PF_{10}-$P2VP_{75}$, which means that PF_{10}-$P2VP_{75}$ possesses better spectral stability at higher temperatures. The enhanced stability is probably due to the fact that the P2VP coil suppresses the formation of excimers in the PF blocks during annealing at high temperatures [40].

4. Conclusions

The synthesis, morphology, and photophysical characterizations of three amphiphilic rod-coil diblock copolymers comprising PF and P2VP with coil chains of various lengths have been demonstrated. A range of morphologies, including spherical, cylindrical, worm-like, dendritic, and large-compound micelles, were observed by varying the coil length and selectivity of mixed MeOH/THF solvents. These morphologies induce considerable variation in the optical absorption, fluorescence, and PL quantum yields of rod-coil diblock copolymers. The degree of hypsochromic shift and PL quenching are enhanced with an increase in the length of the P2VP coil and the proportion of poor solvent, due to H-type aggregation. This indicates that photophysical properties can be manipulated according to the coil length of the P2VP block and the selectivity of solvents. Furthermore, the P2VP segments efficiently suppress the formation of excimers, indicating that the spectral stability of polyfluorene can be improved through manipulation of the architecture of diblock rod-coil copolymers. This study
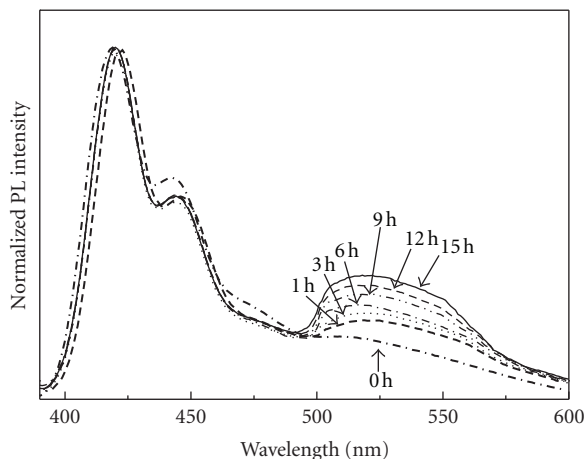
FIGURE 7: Photoluminescence spectra of the thin film of PF macroinitiator annealed at 120°C for 0 h, 1 h, 3 h, 6 h, 9 h, 12 h, and 15 h.
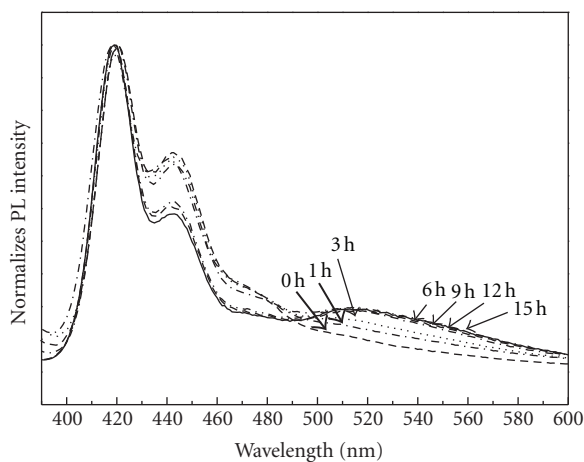

FIGURE 8: Photoluminescence spectra of the thin film of PF macroinitiator, $(PF)_{10}$-b-$(P2VP)_{75}$ annealed at 120°C for 0 h, 1 h, 3 h, 6 h, 9 h, 12 h, and 15 h.

demonstrates the importance of coil length and the selectivity of solvents on the morphology and optical characteristics of rod-coil copolymers. Further, the importance of rod length on the morphology and optical characteristics of rod-coil copolymers will be investigated in our next study.

Acknowledgment

References

[1] A. Hirao, M. Hayashi, S. Loykulnant et al., "Precise syntheses of chain-multi-functionalized polymers, star-branched polymers, star-linear block polymers, densely branched polymers, and dendritic branched polymers based on iterative approach using functionalized 1,1-diphenylethylene derivatives," *Progress in Polymer Science*, vol. 30, no. 2, pp. 111–182, 2005.

[2] P. Chen, G. Yang, T. Liu, T. Li, M. Wang, and W. Huang, "Optimization of opto-electronic property and device efficiency of polyfluorenes by tuning structure and morphology," *Polymer International*, vol. 55, no. 5, pp. 473–490, 2006.

[3] Y. Liang, H. Wang, S. Yuan, Y. Lee, L. Gan, and L. Yu, "Conjugated block copolymers and co-oligomers: from supramolecular assembly to molecular electronics," *Journal of Materials Chemistry*, vol. 17, no. 21, pp. 2183–2194, 2007.

[4] Y. B. Lim, K. S. Moon, and M. Lee, "Rod-coil block molecules: their aqueous self-assembly and biomaterials applications," *Journal of Materials Chemistry*, vol. 18, no. 25, pp. 2909–2918, 2008.

[5] X. Yang, F. Yi, Z. Xin, and S. Zheng, "Morphology and mechanical properties of nanostructured blends of epoxy resin with poly(ε-caprolactone)-block-poly(butadiene-co-acrylonitrile)-block-poly(ε-caprolactone) triblock copolymer," *Polymer*, vol. 50, no. 16, pp. 4089–4100, 2009.

[6] J. F. Gohy, "Metallo-supramolecular block copolymer micelles," *Coordination Chemistry Reviews*, vol. 253, no. 17-18, pp. 2214–2225, 2009.

[7] Y. Wang, M. Zhang, C. Moers et al., "Block copolymer aggregates with photo-responsive switches: towards a controllable supramolecular container," *Polymer*, vol. 50, no. 20, pp. 4821–4828, 2009.

[8] S. W. Kuo, P. H. Tung, and F. C. Chang, "Hydrogen bond mediated supramolecular micellization of diblock copolymer mixture in common solvents," *European Polymer Journal*, vol. 45, no. 7, pp. 1924–1935, 2009.

[9] J. Tata, D. Scalarone, M. Lazzari, and O. Chiantore, "Control of morphology orientation in thin films of PS-b-PEO diblock copolymers and PS-b-PEO/resorcinol molecular complexes," *European Polymer Journal*, vol. 45, no. 9, pp. 2520–2528, 2009.

[10] Y. W. Li, H. Li, B. Xu et al., "Molecular structure-property engineering for photovoltaic applications: fluorene-acceptor alternating conjugated copolymers with varied bridged moieties," *Polymer*, vol. 51, pp. 1786–1795, 2010.

[11] D. Yang, L. Tong, Y. Li, J. Hu, S. Zhang, and X. Huang, "A novel well-defined amphiphilic diblock copolymer containing perfluorocyclobutyl aryl ether-based hydrophobic segment," *Polymer*, vol. 51, no. 8, pp. 1752–1760, 2010.

[12] A. E. Smith, X. Xu, and C. L. McCormick, "Stimuli-responsive amphiphilic (co)polymers via RAFT polymerization," *Progress in Polymer Science*, vol. 35, no. 1-2, pp. 45–93, 2010.

[13] C. L. Liu, C. H. Lin, C. C. Kuo, S. T. Lin, and W. C. Chen, "Conjugated rod-coil block copolymers: synthesis, morphology, photophysical properties, and stimuli-responsive applications," *Progress in Polymer Science*, vol. 36, no. 5, pp. 603–637, 2011.

[14] G. Chang, L. Yu, Z. Yang, and J. Ding, "A delicate ionizable-group effect on self-assembly and thermogelling of amphiphilic block copolymers in water," *Polymer*, vol. 50, no. 25, pp. 6111–6120, 2009.

[15] T. Qu, A. Wang, J. Yuan, and Q. Gao, "Preparation of an amphiphilic triblock copolymer with pH- and thermo-responsiveness and self-assembled micelles applied to drug release," *Journal of Colloid and Interface Science*, vol. 336, no. 2, pp. 865–871, 2009.

[16] H. J. Chung and T. G. Park, "Self-assembled and nanostructured hydrogels for drug delivery and tissue engineering," *Nano Today*, vol. 4, no. 5, pp. 429–437, 2009.

[17] M. Lee, B. K. Cho, and W. C. Zin, "Supramolecular structures from rod-coil block copolymers," *Chemical Reviews*, vol. 101, no. 12, pp. 3869–3892, 2001.

[18] F. J. M. Hoeben, P. Jonkheijm, E. W. Meijer, and A. P. H. J. Schenning, "About supramolecular assemblies of π-conjugated systems," *Chemical Reviews*, vol. 105, no. 4, pp. 1491–1546, 2005.

[19] J. J. L. M. Cornelissen, M. Fischer, N. A. J. M. Sommerdijk, and R. J. M. Nolte, "Helical superstructures from charged poly(styrene)- poly(isocyanodipeptide) block copolymers," *Science*, vol. 280, no. 5368, pp. 1427–1430, 1998.

[20] S. A. Jenekhe and X. L. Chen, "Self-assembled aggregates of rod-coil block copolymers and their solubilization and encapsulation of fullerenes," *Science*, vol. 279, no. 5358, pp. 1903–1907, 1998.

[21] Y. C. Tung, W. C. Wu, and W. C. Chen, "Morphological transformation and photophysical properties of rod-coil poly[2,7-(9,9- Dihexylfluorene)]-block-poly(acrylic acid) in solution," *Macromolecular Rapid Communications*, vol. 27, no. 21, pp. 1838–1844, 2006.

[22] C. H. Lin, Y. C. Tung, J. Ruokolainen, R. Mezzenga, and W. C. Chen, "Poly[2,7-(9,9-dihexylfluorene)]-block-poly(2-vinylpyridine) rod-coil and coil-rod-coil block copolymers: synthesis, morphology and photophysical properties in methanol/THF mixed solvents," *Macromolecules*, vol. 41, no. 22, pp. 8759–8769, 2008.

[23] G. Zhang, D. Wang, and H. Mohwald, "Nanoembossment of Au patterns on microspheres," *Materials Chemistry*, vol. 18, pp. 3985–3992, 2006.

[24] Y. C. Tung and W. C. Chen, "Poly[2,7-(9,9-dihexylfluorene)]-block-poly[3-(trimethoxysilyl)propyl methacrylate] (PF-b-PTMSPMA) rod-coil block copolymers: synthesis, morphology and photophysical properties in mixed solvents," *Reactive and Functional Polymers*, vol. 69, no. 7, pp. 507–518, 2009.

[25] C. A. Dai, W. C. Yen, Y. H. Lee, C. C. Ho, and W. F. Su, "Facile synthesis of well-defined block copolymers containing regioregular poly(3-hexyl thiophene) via anionic macroinitiation method and their self-assembly behavior," *Journal of the American Chemical Society*, vol. 129, no. 36, pp. 11036–11038, 2007.

[26] C. L. Zhu, L. B. Liu, Q. Yang, F. T. Lv, and S. Wang, "Water-soluble conjugated polymers for imaging, diagnosis, and therapy," *Chemical Reviews*, vol. 112, pp. 4687–4735, 2012.

[27] A. Kaeser and A. P. Schenning, "Fluorescent nanoparticles based on self-assembled π-conjugated systems," *Advanced Materials*, vol. 22, pp. 2985–2997, 2010.

[28] R. Abbel, A. P. H. J. Schenning, and E. W. Meijer, "Fluorene-based materials and their supramolecular properties," *Journal of Polymer Science A*, vol. 47, no. 17, pp. 4215–4233, 2009.

[29] J. Zaumseil and H. Sirringhaus, "Electron and ambipolar transport in organic field-effect transistors," *Chemical Reviews*, vol. 107, no. 4, pp. 1296–1323, 2007.

[30] W. C. Wu, W. Y. Lee, and W. C. Chen, "New fluorene-acceptor random copolymers: towards pure white light emission from a single polymer," *Macromolecular Chemistry and Physics*, vol. 207, no. 13, pp. 1131–1138, 2006.

[31] W. C. Wu, C. L. Liu, and W. C. Chen, "Synthesis and characterization of new fluorene-acceptor alternating and random copolymers for light-emitting applications," *Polymer*, vol. 47, no. 2, pp. 527–538, 2006.

[32] G. Bernardo, A. Charas, and J. Morgado, "Luminescence properties of poly(9,9-dioctylfluorene)/polyvinylcarbazole blends: role of composition on the emission colour stability and electroluminescence efficiency," *Journal of Physics and Chemistry of Solids*, vol. 71, no. 3, pp. 340–345, 2010.

[33] Z. S. Guo, J. Pei, Z. L. Zhou et al., "Amine groups-functionalized alcohol-soluble polyfluorene derivatives: synthesis, photophysical properties, and self-assembly behaviors," *Polymer*, vol. 50, no. 20, pp. 4794–4800, 2009.

[34] Y. K. Kwon, H. S. Kim, H. J. Kim et al., "Reduced excimer formation in polyfluorenes by introducing coil-like poly[penta(ethylene glycol) methyl ether methacrylate] block segments," *Macromolecules*, vol. 42, no. 3, pp. 887–891, 2009.

[35] S. Lu, Q. L. Fan, S. J. Chua, and W. Huang, "Synthesis of conjugated-ionic block copolymers by controlled radical polymerization," *Macromolecules*, vol. 36, no. 2, pp. 304–310, 2003.

[36] C. L. Chochos, P. K. Tsolakis, V. G. Gregoriou, and J. K. Kallitsis, "Influence of the coil block on the properties of rod-coil diblock copolymers with oligofluorene as the rigid segment," *Macromolecules*, vol. 37, no. 7, pp. 2502–2510, 2004.

[37] S. Lu, T. Liu, L. Ke, D. G. Ma, S. J. Chua, and W. Huang, "Polyfluorene-based light-emitting rod-coil block copolymers," *Macromolecules*, vol. 38, no. 20, pp. 8494–8502, 2005.

[38] D. Marsitzky, M. Klapper, and K. Müllen, "End-functionalization of poly(2,7-fluorene): a key step toward novel luminescent rod-coil block copolymers," *Macromolecules*, vol. 32, no. 25, pp. 8685–8688, 1999.

[39] J. F. Gohy, H. Hofmeier, A. Alexeev, and U. S. Schubert, "Aqueous micelles from supramolecular graft copolymers," *Macromolecular Chemistry and Physics*, vol. 204, pp. 1524–1530, 2003.

[40] Y. K. Kwon, H. S. Kim, H. J. Kim et al., "Reduced excimer formation in polyfluorenes by introducing coil-like poly[penta(ethylene glycol) methyl ether methacrylate] block segments," *Macromolecules*, vol. 42, no. 3, pp. 887–891, 2009.

Journal of
Nanotechnology

International Journal of
Corrosion

International Journal of
Polymer Science

Smart Materials
Research

Journal of
Composites

BioMed
Research International

Journal of
Metallurgy

Journal of
Materials

Hindawi

Submit your manuscripts at
http://www.hindawi.com

Journal of
Nanoparticles

Advances in
Materials Science and Engineering

Scientifica

Journal of
Nanomaterials

The Scientific
World Journal

International Journal of
Biomaterials

Journal of
Nanoscience

Journal of
Coatings

Journal of
Crystallography

Journal of
Ceramics

Journal of
Textiles